Journal of Materials Science & Nanotechnology
Volume 10 | Issue 1
ISSN: 2348-9812

Research Article Open Access

Evaluation of Characterization Results of Ru, Sb And V_Doped Sno$_2$ Coatings Deposited by Using Produced and Commercial Targets

Anli ST[1*], Ebeoglugil MF[2]

[1]Department of Metallurgical and Materials Engineering, Dokuz Eylul University, Buca, Izmir, Turkey, 35900, Turkey
[2]Department of Metallurgical and Materials Engineering, Dokuz Eylul University, Buca, Izmir, Turkey, 35900, Turkey

Corresponding author: Anli ST, Department of Metallurgical and Materials Engineering, Dokuz Eylul University, Buca, Izmir, Turkey, 35900, Turkey. Tel: 0(507) 980 82 19, Email: sehertas35@yahoo.com

Citation: Anli ST, Ebeoglugil MF (2022) Evaluation of Characterization Results of Ru, Sb And V_Doped Sno2 Coatings Deposited by Using Produced and Commercial Targets. J Mater Sci Nanotechnol 10(1): 103

Abstract

Ruthenium, Antimony and Vanadium doped and undoped tin oxide (SnO_2) thin films were prepared by the R.F. Sputtering method. At the beginning of the thin film production studies, pellets were formed by pressing the filled and undoped tin oxide powders in the laboratory environment. The purpose of creating these pellets is to replace commercially purchased target material that acts as the coating material in the sputter coating device. The aim of the study is to use these pellets instead of this commercial target due to its disadvantages such as long lead time and expensiveness, and thus to produce easier, more diverse and high quality thin films. This study includes the synthesis of pure and doped thin films of tin oxide semiconductor material, which has a wide band gap and attracts attention with its wide spread use thanks to this feature, subjecting it to annealing process under different temperatures and times, and structural and morphological characterization studies: XRD, SEM, AFM, XPS, UV-Vis Spectrophotometer and Nano-hardness machine.

The study showed that doped and undoped tin oxide films showed similar properties to similar studies seen in the literature, so that the pellets formed in the laboratory environment functioned. No major structural difference was observed in the films produced as a result of the use of pellets and target. As a result of the findings of the study, it has been seen that it is a preliminary study for the investigation of gas sensing properties.

Keywords: Doped, Pellet, SnO_2, Sputtering, Target, Thin film, Tin Oxide

Introduction

Recent advences in nanotechnology increase the importance of semiconductor sensors in the electronics industry. Thanks to its low-cost production and stable structure [1,2], semiconductor thin film makes its use in microelectronics advantageous, and the interest in academic publications on this subject continues with new developments [3,4]. SnO_2 is IV-VI group compounds, it is an n-type semiconductor material with a wide energy band gap (eg ~3.6-4 eV) at room temperature [5]. These properties of tin oxide provide low electrical resistance, optical transmittance, high chemical, thermal and mechanical stability when tin oxide is coated on various substrates as a thin film [6]. The good adhesion of tin oxide films to various surfaces and their resistance to adverse environmental effects make it useful in many application areas. These thin films are widely preferred for solar cells, electrodes[1,7,8], magnetic recording devices, as well as especially in the field of gas sensor applications due to their high gas detection sensitivity to gases [3,9-11]. The structural and chemical properties of SnO_2 thin films vary depending on the experimental parameters, additives and production techniques applied in their production [8,12-15]. With the addition of some elements (Ru, Sb, V, Mo, Cu, Cr, Pt, Pd, In...) to pure tin dioxide [13,16-18], a tremendous change in electrical properties is observed, providing important data sources in this respect. [7,8]. Thanks to the use of advanced coating production methods, films can be easily coated on various surfaces (silica, glass), providing a good adhesion between the substrate and the coating, thus technical reliability is achieved in coatings.

SnO_2 thin films can be prepared by various methods such as Sputtering [5,9,10,19,20], Pulsed Laser Deposition (PLD) [19] and Sol-gel process [1,11,21]. The sputtering method offers advantages compared to other deposition techniques in terms of being able to work at low substrate temperatures, high deposition rate, easy control of film thickness, and being economical [9]. The disk-shaped so-called target material used as the coating material in this technique is often commercially costly. The expected properties of the target material are low pollution, high purity, homogeneous (texture, grain size, precipitate, crystallite), dense, durable, non-porous [7]. To form a stable film, the target material must have a density close to its theoretical density. Dense ceramic targets have higher resistance to spray erosion and nodule formation.

In this article, the production of doped and undoped SnO_2 tin oxide thin films on silica substrate using Sb, V and Ru doped and undoped target materials by RF (Radio Frequency) sputtering method is presented. Electrical, structural, mechanical and morphological examinations were performed depending on different time and calcination temperatures and additive elements to compare the films produced using purchased pure and laboratory-produced pure and doped tin oxide targets. Properties of oxide thin films (XRD), Scanning Electron Microscopy (SEM), Atomic Forrier Transform (AFM) and X-Ray Photoelectron Spectrum (XPS), UV-Vis Spectrophotometer and Nano-hardness machine were performed.

The work was carried out in the following order: First, tin oxide films of 50, 100 and 200 nm thickness without additives were produced from commercial and laboratory produced targets. These films were annealed at different temperatures at different times and XRD (Figure 1), SEM and AFM comparisons were made (Figures 10, 11). Then, thin films were produced from the doped pellets. XRD analyzes of doped and undoped films are presented in a single graph (Figure 2) and XPS analyzes are presented in separate graphs (Figure 3, 4, 5, 6, 7). SEM and AFM graphs of unadulterated films are given in Figure 8 and Figure 9. The hardness and optical band gap of doped and undoped films are presented in Figure 11 and Figure 12, respectively.

This study considers the stability of the structural and electrical properties of the films and tries to compare the properties of the films produced by the mentioned methods. In addition, the questioning of the usability of the pellets produced in the laboratory as a target for coating films, the deadline, and the high cost effect of especially the element-added targets are among the main reasons for the research.

Materials and Methods

Preparation and Chacterization Studies of Doped and Undoped Sno$_2$ Films

Undoped and doped films were coated on the silica substrates using purchased (99.98 % pure, 2.00" diameter x 0.250" thick) tin oxide target and lab-made undoped, Antimon Sb-, V-, Ru- doped SnO_2 pellets in the RF Sputteringdevice. Manufacture of doped and undoped SnO_2 pellets were from its powders from synthesizing with the pure and each by dopant ruthenium, antimony, vanadium nanocrystalline using sol-gel method, which production is described in under condition of laboratory [22].

Pellets were prepared by giving the shape of a disc by pressing from 2.0 wt.% Ru, 2.0 wt% V, 2.0 wt% Sb doped and undoped SnO_2 powders, which is production details were given in the previous article[22]. This work is related to the field of powder metallurgy. PVA (0.5%) binder solution was sprayed on SnO_2 powders, these powders were poured into the mold in an automatic hydraulic press and preformed, so that raw discs were obtained. 5.2 cm diameter and 5 mm thickness pellets were produced by pre-pelleting the powders under 150 bar pressure in automatic pressing. Then, in order to give density to the pellets, the pellets were pressed in a CIP (Cold Isostatic Pressing) device under a pressure of 300 MPa and sintered at 1450 °C 120 min. at 10 °C/min heating rate by passing oxygen (O_2) gas in the tube furnace. Pellets densities were determined using the archimedes method. Their microstructures were examined with the scanning electron microscope (SEM) in the department laboratory by surfaces of the pellet samples taken into resin mold for microscopic examinations were sanded with SiC sandpaper and polished with 3 μm diamond paste and covered with gold. Pure and doped SnO_2 films were prepared by the R.F. Sputtering method by using these doped and undoped (2 at%) SnO_2 pellets (Lab.-made). SnO_2 thin films were deposited on silica substrates at rate of 0.9-1.1 Å/sec with a sputtering power of about 45-55 W and working pressure at 1-1.5 10-2 Torr (1-1.5 mTorr). Here, Å unit corresponds to a metric measure of 0.1 nm. The litter temperature in operation is around 45 °C. Only argon (Ar) gas was used as the operating gas. The distance between substrate and target is kept 6 cm in the chamber. 1x1 and 2x1 cm section silica were used as substrate. The substrate was cleaned by washing in the ultrasonic device, rinsing with deionized water and drying at 105 °C [6]. Undoped tin oxide film samples produced were subjected to annealing at 550 °C - 650 °C and 45-120 minutes in air atmosphere. Ru, Sb, V doped tin oxide films annealed for 120 min at 650 °C air atmosphere to ensure oxidation.

Characterization Techniques

Structural properties of pure and doped SnO_2 films were characterized by XRD, XPS, AFM, SEM, UV–Vis and Nanohardness. The crystalline structure was examined by X-ray diffraction (XRD) (Rigaku, Dmax2200) using CuKα radiation. The analyzes were performed under CuKα radiation at 1.54 Å wavelength with voltage and current settings of 45 kV and 44 mA. For qualitative analysis, XRD diagrams were recorded scan range 20° to 80° in 2θ angles and the scan step was 2°/min. The morphological features of thin films were characterized by using scanning electron microscopy (SEM) (JEOL JSM 6060, Japon). SEM imaging was perrformed accelerating voltage of 5-20 kV. Before the analysis, the surfaces of the films were coated with gold to capture better resolution. All samples were examined under 1000X-5000X magnification and subsequently focused higher magnifications to obtain more details from the samples.

Topographies and roughness of the films were carried out using a atomic force microscopy (AFM, Nanosurf Flex Axiom). All AFM measurements were performed in ambient conditions. Three measurements were performed for each specimen. The measured roughness parameters were Ra (arithmetic average roughness), Rq (root-mean-square) and Rt (maximum height of the profile). The surface chemical composition was identified by X-ray photoelectron spectroscopy (XPS, Thermo Scientific, UK) with monochromatic Al Kα (1486.6 eV). X-ray source and a beam size of 400 nm diameter. Chamber pressure during XPS analyses was kept lower than 10^{-9} Torr. Survey XPS data were acquired to 1350 eV from 10 eV with pass energy of 50.0 eV and a energy step size of 0.1 eVand spot size of 400 μm. The spectrometer was calibrated according the Au 4f peak of pure gold. Surfaces of all samples before operation were sputtered with ionic argon gas. Binding energies and atomic concentration ratios were obtained using the curve fitting software implemented in the Advantage software program provided by the device manufacturer (Thermo Scientific, UK).

Thickness measurement of thin films surface profilometer [8], optical microscope and surface nanohardness (nanoindentation) measurement tests for mechanical measurements [23] and band gap tests for electrical measurements were performed [24]. The films thicknesses was measured by contact method (Mitutoyo SJ-301).

Their optical properties were investigated using UV–Visible spectrophotometer (Thermo UV-1240 Shimadzu UV/VIS) at wavelength range of 190 to 900 nm to calculate the band gap of the films.

Results and Discussions

XRD Analysis

Phase analysis of all doped and undoped tin oxide thin films were obtained from X-Ray Diffraction (XRD). Figure 1 shows a phase analysis study (XRD) to compare the calcination temperature and time of pure tin oxide thin films of 200 nm thickness produced using a commercially purchased target. Pure SnO_2 films annealed at two different temperatures were prepared. XRD studies reveal a tetragonal rutile crystalline phases of tin oxide.

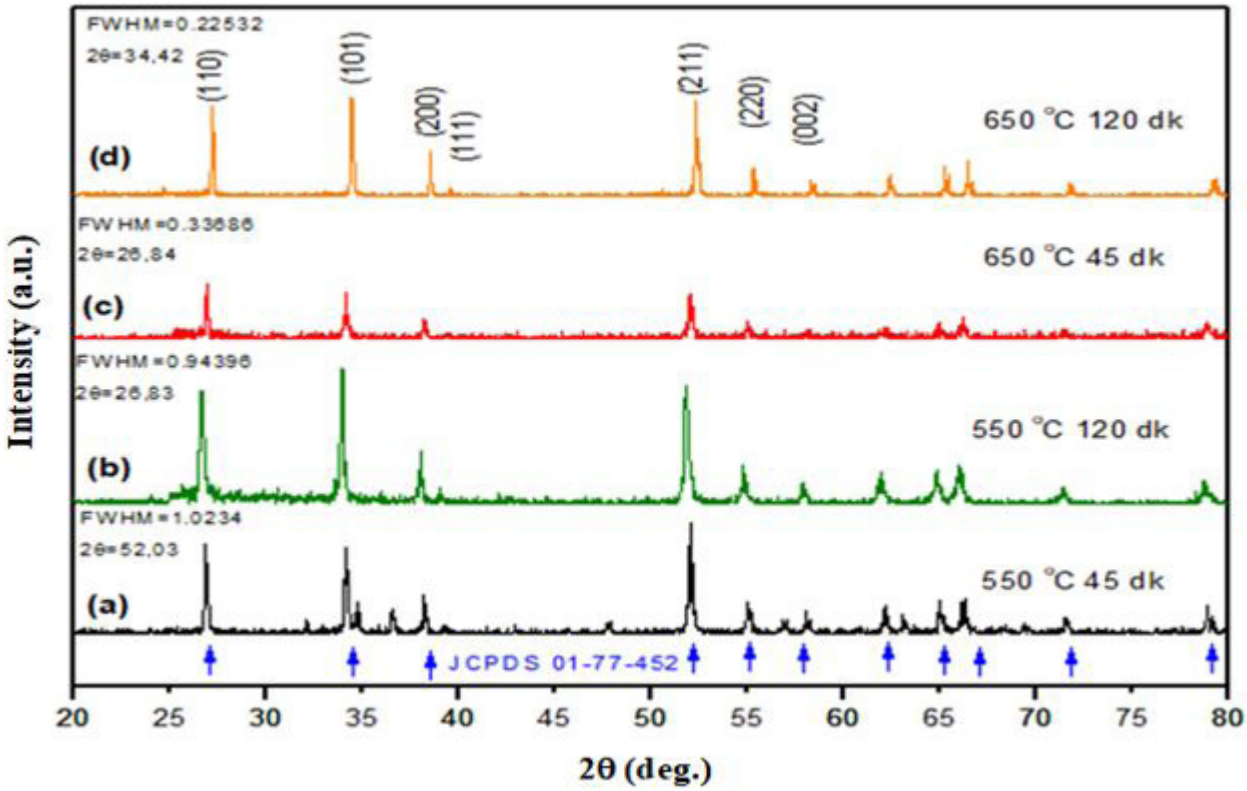

Figure 1: XRD spectrum of pure SnO_2 thin films of 200 nm thickness produced with a purchased SnO_2 target annealed at (a) 550 °C, 45 min. (b) 550 °C, 120 min (c) 650 °C, 45 min (d) 650 °C 120 min

The XRD diffraction patterns of the films annealed at 550 and 650 °C for 45 and 120 minutes times show that all films are polycrystalline and the peak characteristics of SnO_2 tetragonal structure. XRD results reveal a tetragonal rutile crystalline phases of tin oxide. The annealed films showes preferential orientation in the characteristic peak positions hkl (Miller indices) (110), (101), (200), (211), (220), (002), (310) and (202) planes. After annealing at 550 °C, it shows a weak (101) peak for the tin oxide phase, but the intensity of this peak increases as the annealing time increases. The densest peaks are seen in the (110), (101) and (211) planes. The width of the peaks indicates that the existing films are composed of tiny nanoparticles. The diffraction peaks of the sample change significantly after the annealing temperature is raised to 650 °C. From the Debye-Scherrer formula ($D = k\lambda / \beta\cos\theta$) the crystal dimensions are calculated. Crystal size (D) was calculated using. In the formula, D is the crystalline size. Where k is the shape factor that takes a value

of about 0.9, λ is the wavelength of the X-ray source used, (FWHM) is the full width at half maximum and θ is the Braggs diffraction angle. Average crystal sizes in these films are on the nanometer scale and are estimated to be about 7 nm to 15 nm. In Figure 1, crystal sizes (*D*), from (a) to (d) are respectively 9,03 nm, 9.04 nm, 25.40 nm, while it was calculated as 39.55 nm. Crystal sizes can be explained as increasing with a cumulative effect of temperature and time. Figure 2 shows the XRD diffraction patterns of undoped and Sb, V and Ru doped tin oxide films, which produced with the lab-made target and purchased target. The diffraction peaks coincided with the casitterite (JCPDS Card No. 01-077-0452) phase. According to XRD patterns, undoped and doped SnO_2 filmss exhibited the typical rutile-type tetragonal structure of SnO_2 with average crystallite sizes for each ranging from 8 to 4 nm when the element content. The size of the crystalline can be estimated by whether the X-ray diffractions are sharp or wide. It has been observed that the additive elements affect the peak intensity and density, thus the crystalline size. The crystal size of doped and doped tin oxide films tended to increase with the addition of Ru and Sb, while remaining the same with the V doping. The average crystalline particle sizes is decreased by increasing the vanadium dopant concentration according Reddy et al. The ionic radii are respectively: 0.71Å for Sn4+, 0.64Å for V^{3+}, 0.58 Å for V^{4+} and 0.54 Å for V^{5+}. The vanadium addition caused a small increase in peak density. This situation indicates that vanadium is a caliper atom in the SnO_2 lattice, due to V cations with smaller ionic radii than Sn^{4+} ion. The addition of ruthenium resulted in an ionic radius of 0.68 Å for Ru^{3+} and a magnitude of the same radii as for Sn^{4+}. By the antimony addition, the atoms are thought to form a structure, mostly in place of the tin atom or in the cage. The Sb cations with an ionic radius of 0.61Å for $Sb^{5+}$and 0.76Å for Sb^{3+} caused a slight increase in the size of the crystalline. Crystallization and growth of SnO_2 were inhibited as Sb amount increased. Zheng et al. emphasized that the crystallization and growth of SnO_2 was inhibited as the amount of Sb addition increased. Reddy et al. noticed that the average crystalline particle size decreased with increasing vanadium doping concentration. The displacement of the doping ions in the Sn^{4+} region is not expected to cause any significant distortion because it is almost identical in ionic radii. However, a slight change to higher angles was observed for V doped tin oxide peaks compared to the peaks of Sb doped tin oxide. However, it was observed that the substitution of V, Ru and Sb ions in the cassiterite lattice did not change the undoped tin oxide cassiterite structure. (110) the main peak shifted slightly towards lower angles with increasing concentration of V^{4+} (0.710) Å ions, This means that the unit cell grows larger because the ionic radius of V^{4+} is slightly larger than the other additives.

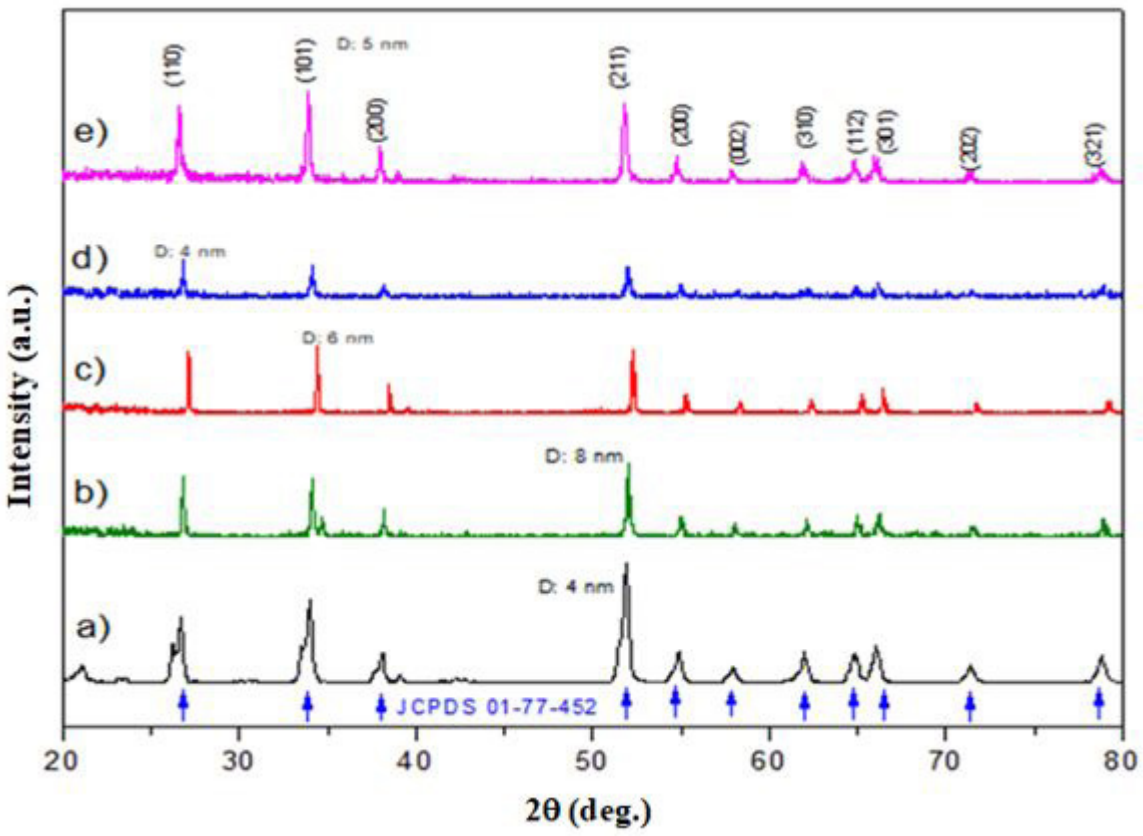

Figure 2: XRD spectrum of annealed SnO_2 thin films produced using laboratory produced targets (a) undoped SnO_2 c) Ru-doped SnO_2 d) V-doped SnO_2 e) Sb-doped SnO_2 and using (b) purchased pure SnO_2 target

XPS Analysis

XPS measurements were carried out to determine the surface chemical composition and the oxidation states of the ruthenium, antimony and vanadium doped and undoped tin oxide films (Figures 3, 4, 5, 6,7) using produced laboratory pellets and commercially purchased target. Relative atom concentrations (at. %) and binding energies of the all samples are summarized in on the Survey and high-resolution data of the all of tin oxide film samples [10]. XPS analysis of 200 nm SnO_2 film produced using commercially purchased target is shown in Figure 3. After analyzing the result, it was determined that there are Sn, C and O elements belonging to the undoped tin oxide. Sn3d5/2 (486.6 eV), O1s (531.08 eV) and C1s (285.84 eV) (Sn metal-oxide) structures were observed. The binding energy (BE) tin oxide (SnO_2) has been reported in the literature between 284.8 and 285.2 eV. XPS analysis of 200 nm SnO_2 films produced using undoped tin oxide pellets created under laboratory conditions is shown in Figure 4. As a result of the analysis, it was determined that there are Sn, C and O elements belonging to pure tin oxide. Sn3d5/2 (487.4 eV), O1s (531.85 eV) and C1s (285.94 eV) values are observed.

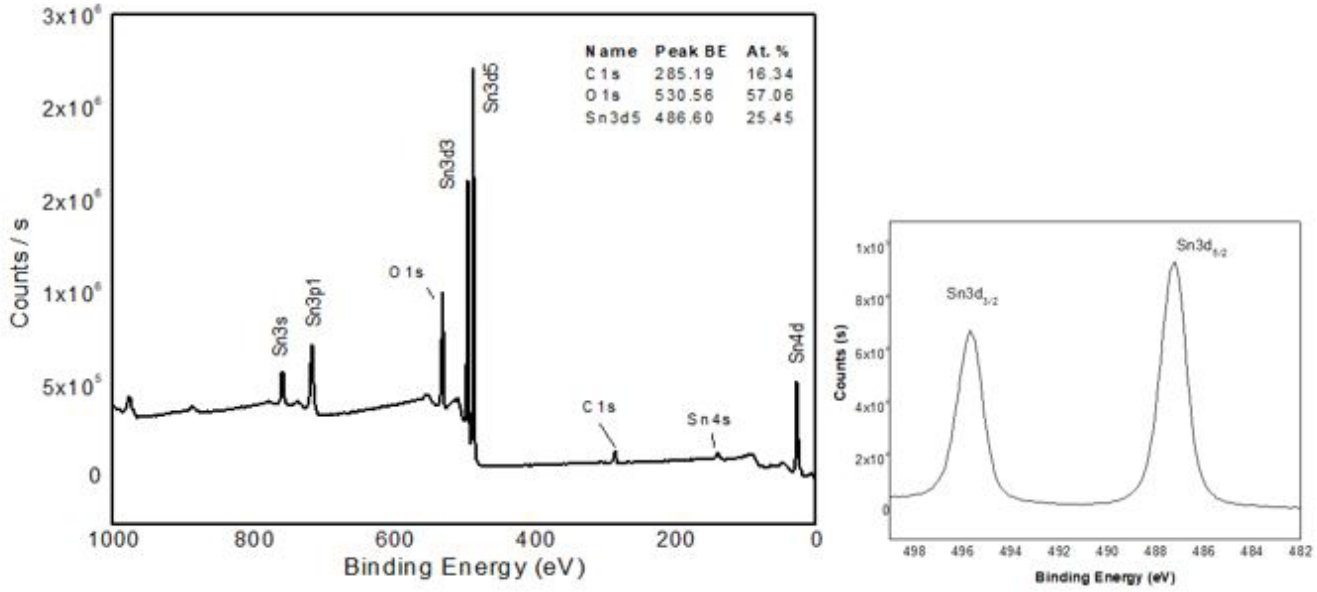

Figure 3: XPS survey and Sn3d high resolution spectrum of tin oxide film produced using the purchased of undoped SnO_2 target

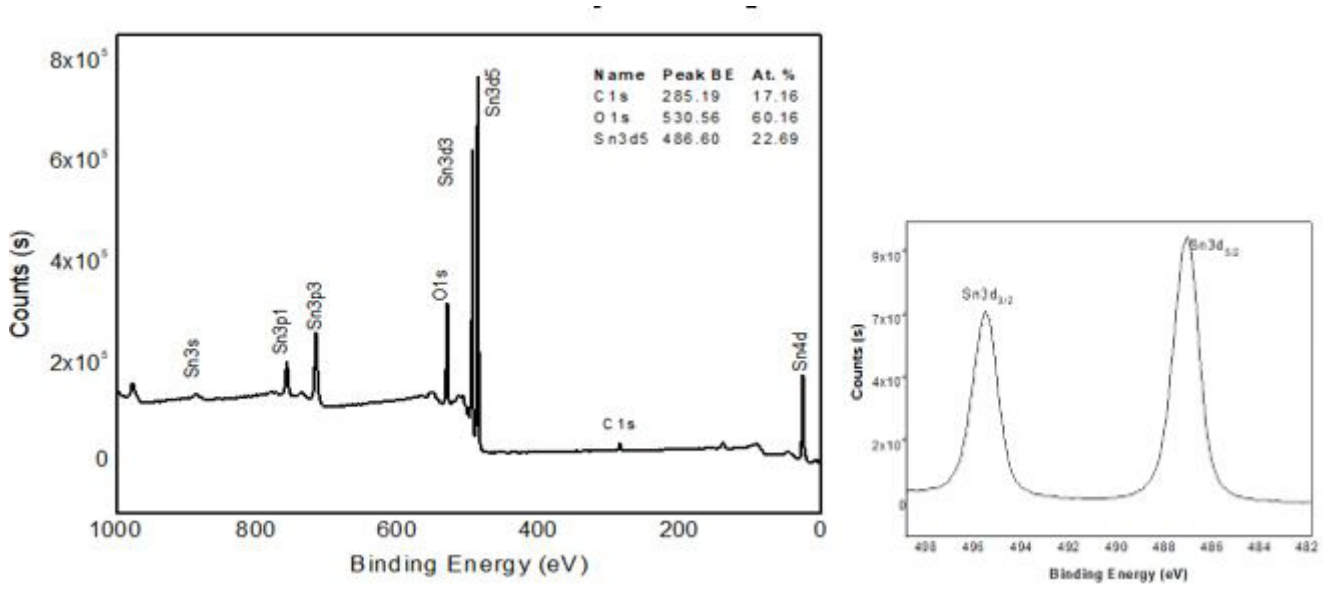

Figure 4: XPS survey and Sn3d high resolution spectrum of deposited tin oxide film using an undoped SnO_2 target produced in the laboratory

XPS elemental analysis graph of ruthenium-doped SnO_2 films is shown in Figure 5. It was seen that the photoelectron peaks coincided for Ru3d (285.28 eV) and C1s (285.38 eV), respectively. There is strong overlap between the Ru3d and C1s regions from RuO_2. XPS elemental analysis graphic of antimony doped SnO_2 films is given in Figure 6. The Sb element also behaved similarly to Ru, coinciding with O1s. Looking at the elemental analysis of this film, it is seen that the photoelectron peaks were overlapping Sb3d (531.35 eV), which chemical state is Sb_2O_3 and Sb_2O_5 and O1s (531.28 eV), respectively. XPS elemental analysis graph of vanadium doped SnO_2 films is given in Figure 7. XPS spectroscopy reveals the presence of three different positions for V+ species. Reddy at all. reddy et al. interpreted the same in their study. Likewise it is seen that V2p (517.4 eV) photoelectron peak values from V_2O_5. V(II) and V(IV) referenced to V2p metal peak. O1s and V2p are located in overlapping regions.

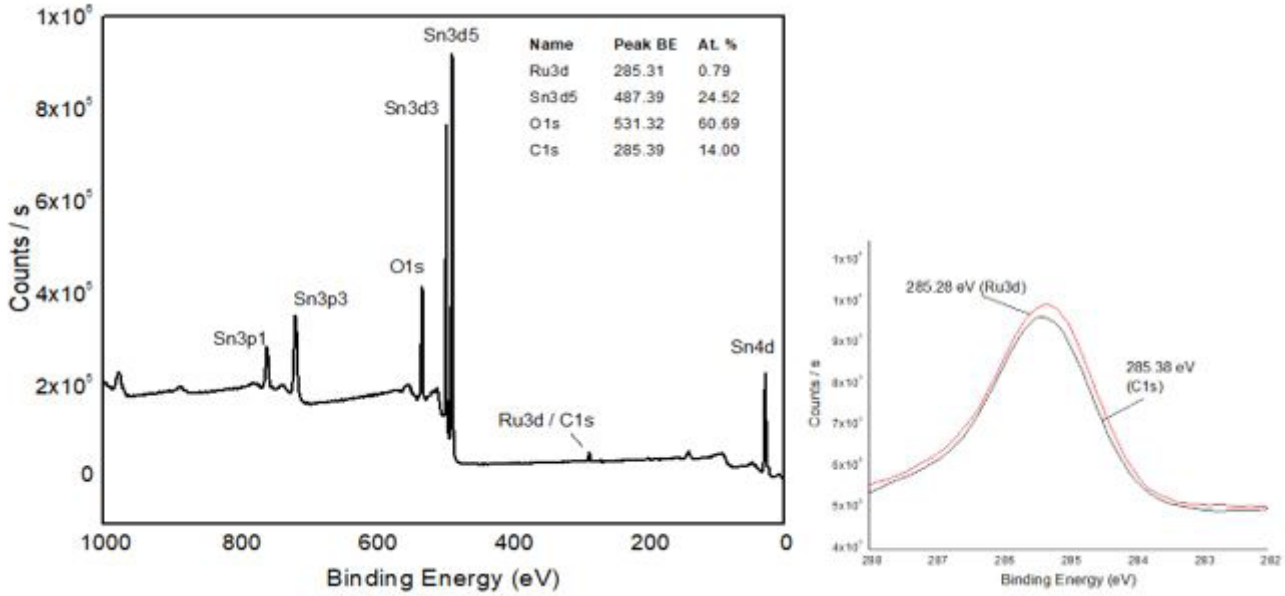

Figure 5: XPS survey and Sn3d high resolution spectrum of deposited tin oxide film using an undoped Ru/SnO_2 target produced in the laboratory

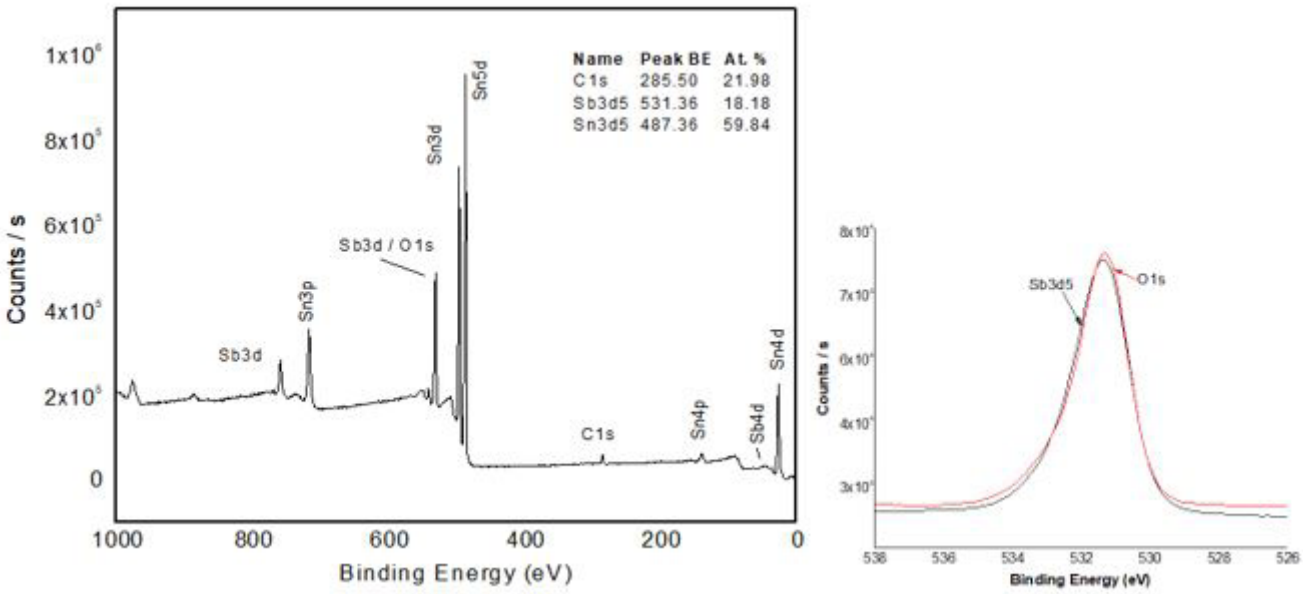

Figure 6: XPS survey and Sn3d high resolution spectrum of deposited tin oxide film using an undoped Sb/SnO_2 target produced in the laboratory

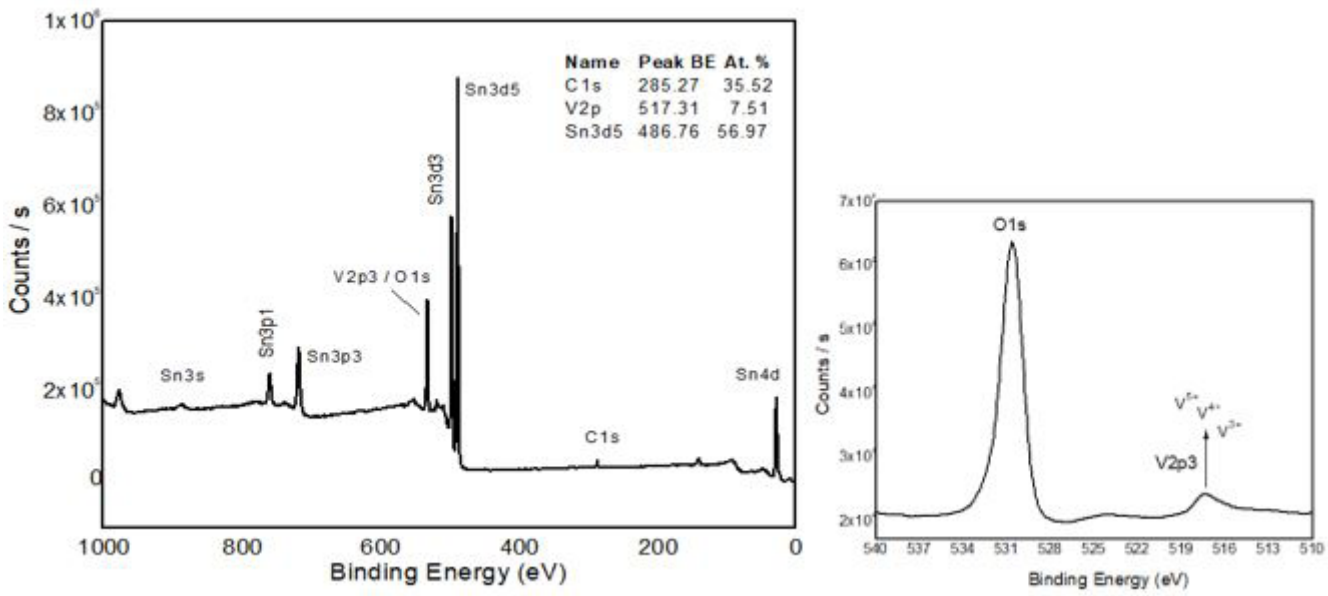

Figure 7: XPS isurvey and Sn3d high resolution spectrum of deposited tin oxide film using an undoped V/SnO_2 target produced in the laboratory

We can conclude that carbon (C) seen in all elemental analyzes is formed as hydrocarbon compounds (seen as standard) as a result of contamination on the surface. The binding energies of the valence bands (Sn3d and O1s, C1s, V2p, Ru3d, Sb5d) of the films are given in tables on the graphics. In the graphics of all these films, the bonding energies of the orbitals of the additives were seen. $Sn3d_{3/2}$ and $Sn3d_{5/2}$ peaks of the two symmetrical spin-orbit pairs in very low Sn3d levels in all films were observed to have energies of 496 and 487 eV. It has been observed that the difference between both core levels is around 9 eV.

The high resolution XPS spectra of the O1s level, which is seen the same in the graphs of all film samples, give a peak point at a binding energy of around 531 eV. These peaks can be attributed to Sn-O in SnO_2 and to the hydroxyl group (C-C, C-O, C=C). Compared to the neat sample, the data clearly show the effect of additives on Sn3d binding energies. These additives mean that the SnO_2 semiconductor can change the Fermi level. Sb, V contributions raise the fermi level as donor. The Ru additive permanently raises the Fermi level down.

Morphology of the Structure (SEM, AFM)

SEM and AFM images were taken to examine the surface morphology and surface roughness of the tin oxide films produced with commercially purchased target material and pellets created under laboratory conditions and with ruthenium, antimony and vanadium additives. The scanned area in AFM is 2x2 μm and 5x5 μm in size. SEM images of pure tin oxide films produced with pellets produced in commercial target and laboratory environment with thicknesses of 50, 100 and 200 nm, respectively, are given in Figure 8. There was no significant difference in grain size and surface appearance between films. While the particle size distribution of the films produced with the commercial target was 10-20 nm in the 100 nm scaled SEM image, the particle size distribution of the films produced with the laboratory pellet was 20-40 nm in the 200 nm scale SEM image. Grain sizes are in the range of 10-40 nm for all films

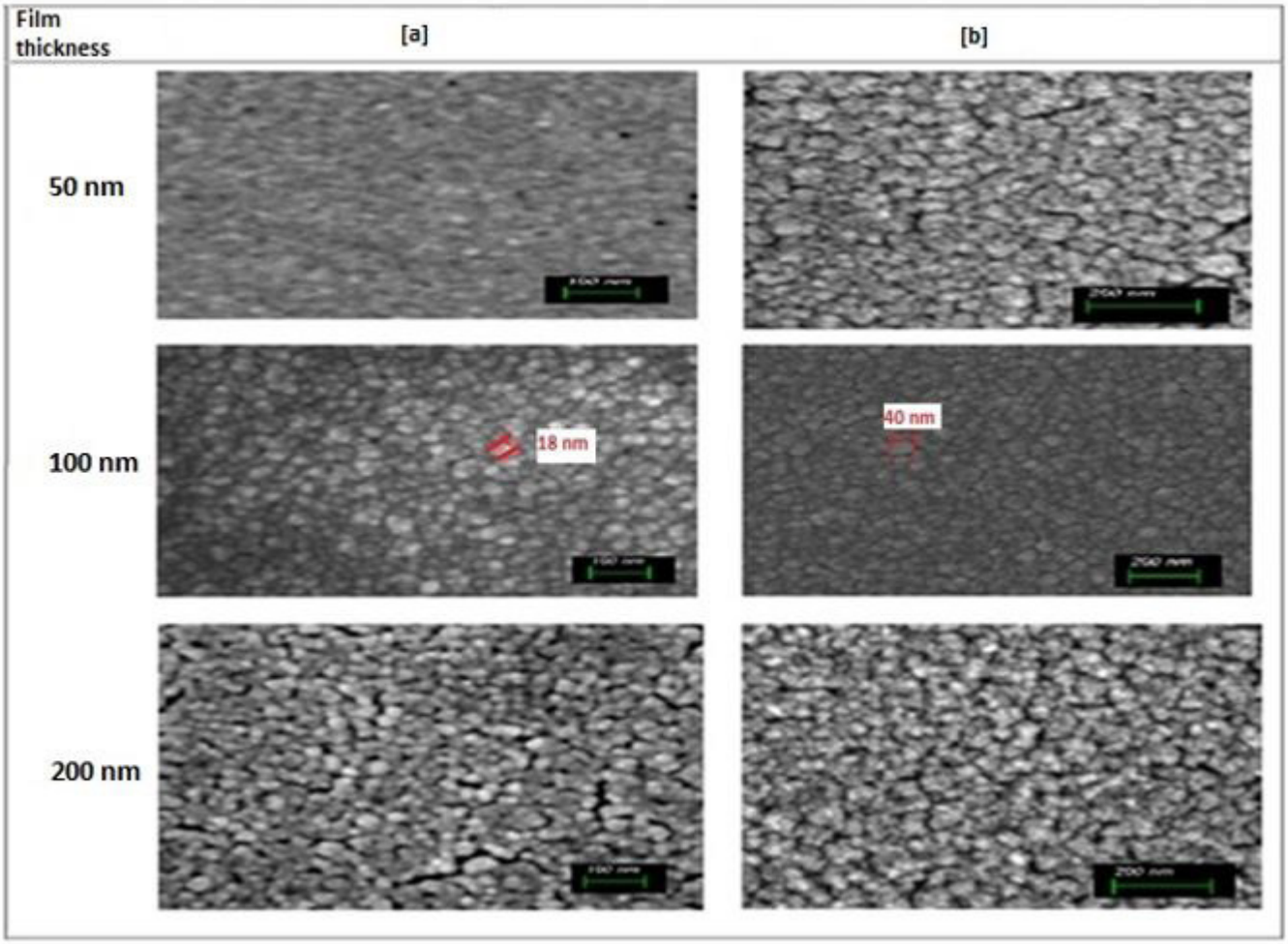

Figure 8: SEM image of pure tin oxide films produced in thicknesses of 50, 100 and 200 nm a) using the purchased SnO_2 target b) using the SnO_2 target produced in the laboratory

In Figure 9, AFM images are seen by scanning an area of 2 x 2 μm of SnO_2 thin films of 50 and 100 nm thickness, which are formed from commercial and laboratory production targets, respectively. AFM images of the film samples showed almost the same topography, and it was observed that the surface topography is not dependent on thickness [5]. Surface roughness values for films produced from pellets formed in the laboratory environment are for 50 nm thickness 13.68 nm, 8.22 nm for 100 thickness films. The roughness values of films produced with commercial targets increased from 9.22 nm for the thickness of 50 nm to 7.44 nm for the thickness of 100 nm.

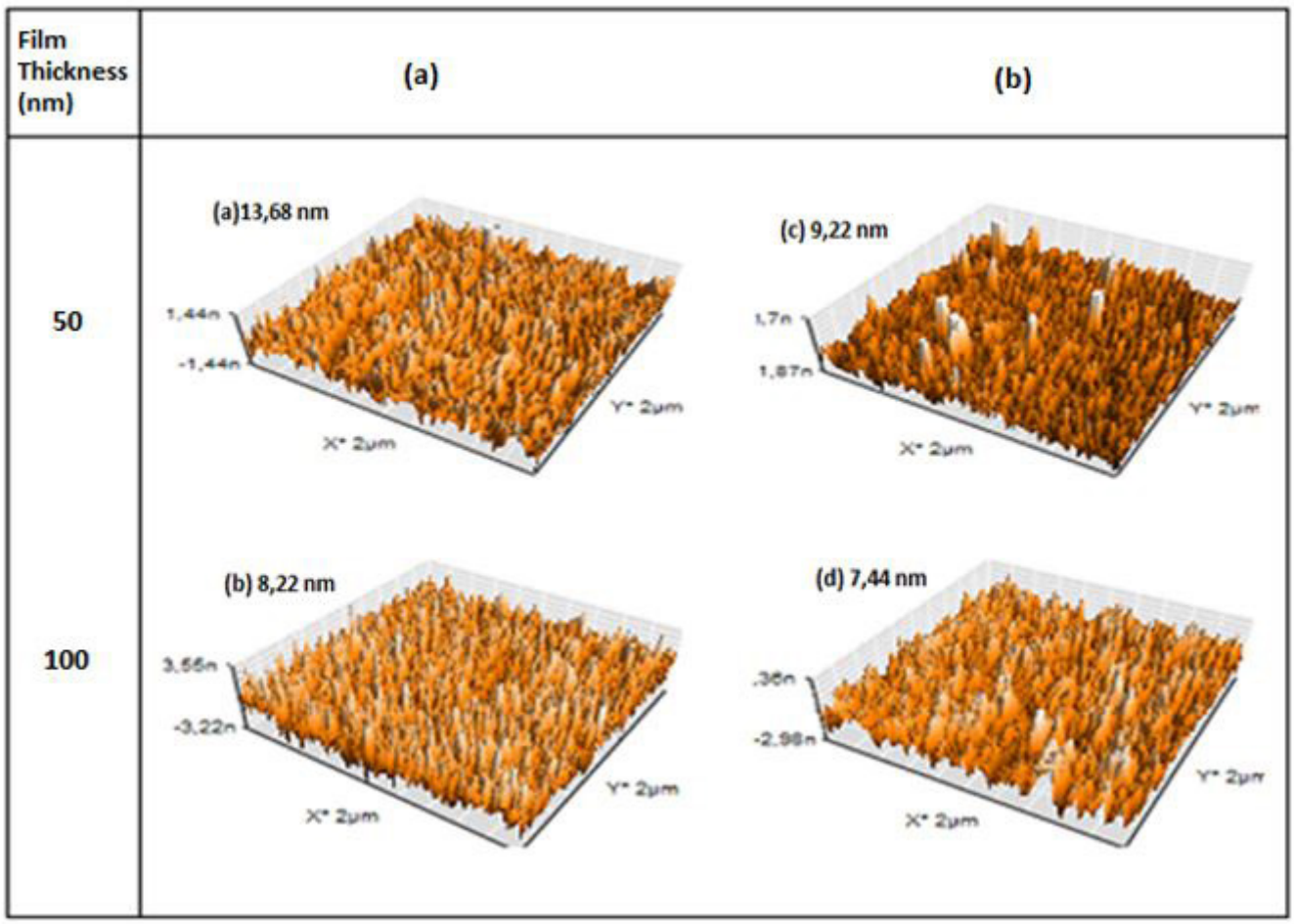

Figure 9: AFM micrographs of pure tin oxide films produced in thicknesses of 50 and 100 nm a) using laboratory produced target b) using purchased target

In Figure 10, SEM and AFM (5x5 µm) images of the 200 nm thickness SnO_2 thin films are annealed at 550 °C and Figure 11 at 650 °C, at 45, 75 and 120 minutes. The films appear to be relatively dense and crystalline grains. It has been found that in these films a roughness increases with increasing annealing temperatures and times. In Figure 10, the surface roughness values for films of 200 nm thickness annealed at 550 °C are between 12-16 nm, respectively. In Figure 11, the surface roughness values for films annealed at 650 °C are in the range of 15-26 nm for 45, 75 and 120 minutes, respectively.

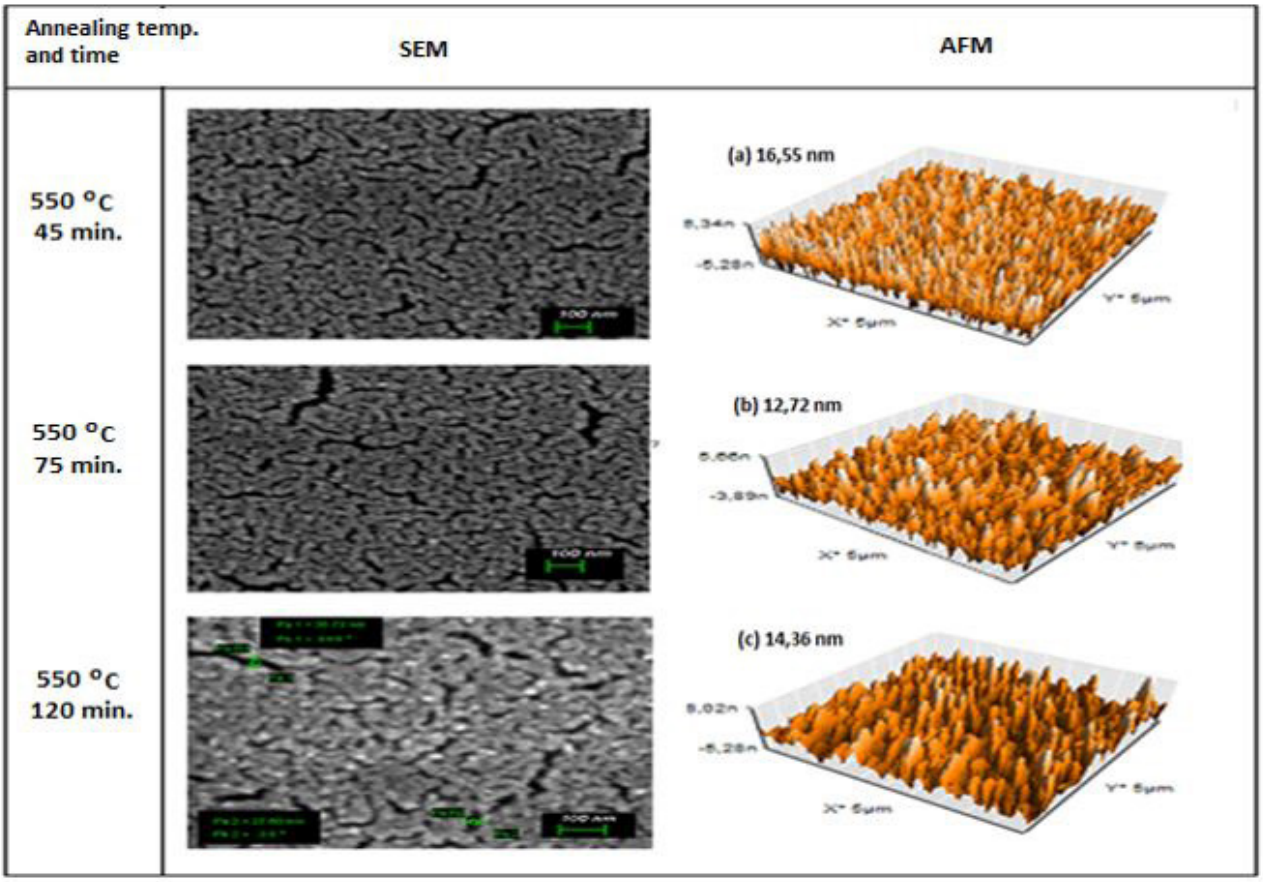

Figure 10: SEM and AFM images of annealed undoped SnO_2 films at 550 °C (a) 45 min (b)75 min (c)120 min

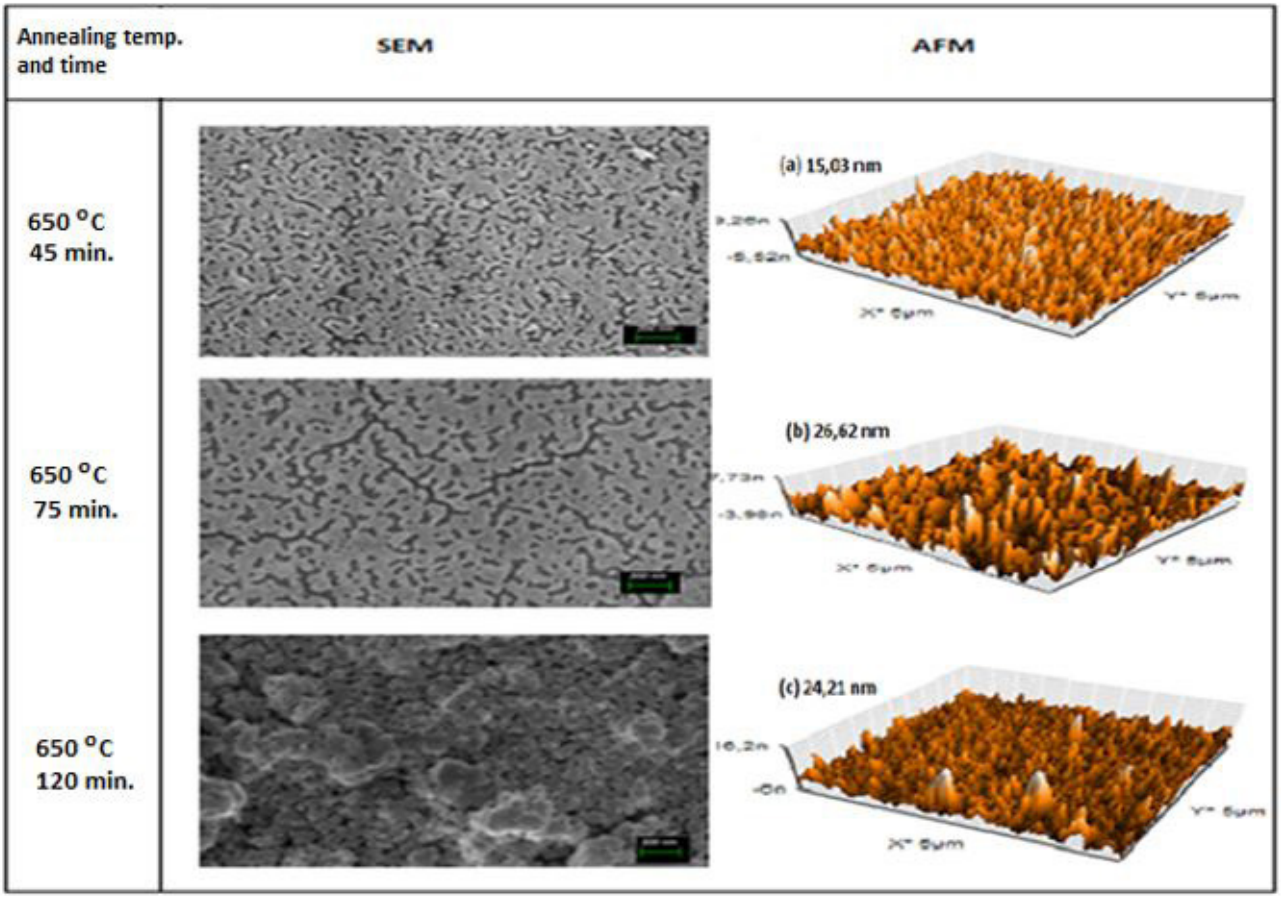

Figure 11: SEM and AFM images of annealed undoped SnO_2 films at 650 °C (a) 45 min (b)75 min (c)120 min

In addition, from the SEM images of Figures 10 and 11, it are seen that annealing process and time have a significant effect on the surface morphology of tin oxide thin films. As the annealing time and temperature increases, coarsening, surface roughness and the grain size increases. the average particle size is about 20 nm at 550 °C. It is increased to 650 °C, the particle size is over 100nm with the combination of small particles. In other words, aggregation is observed in the grains at high annealing temperatures [10, 27]. Therefore, SEM results and XRD results are consistent. There is no significant increase in grain size with the increase of annealing times at the same temperature. However, the SEM images (Figure 11) taken in the film samples annealed at 650 °C for 120 minutes showed better surface roughness with increasing grain growth. According to the result obtained from the SEM images, this temperature and time increase in the SnO_2 concentration with the increase of surface roughness and the formation of larger crystals.

Mechanical Properties

Nanoindentation test was performed for nanomechanical measurement for doped and undoped tin oxide films of 50-100 and 200 nm thickness, hardness (H) and elasticity (Young's) modulus (E) values were obtained depending on the applied load (P). Nanoindentation tests [24, 28], based on the indenter penetration depth between 10-15% of the coating thickness 0.1, 0.2, It was carried out under loads as low as 0.3 and 0.5 mN. Samples were measured at different penetration depths ranging from 0.0073 to 0.0318 μm. The hardness and elastic modulus results of the coatings of all samples and the indentation load (mN) and penetration depth (μm) applied to each sample are as shown in Table 1. Here coding is done. They are coded as SnO_2 thin films T50, T100, T200 and L50, L100 and L200 of 50, 100 and 200 nm thickness, produced with the pure commercial target and undoped laboratory production pelet respectively. Vanadium, antimony and ruthenium doped 200 nm thickness SnO_2 thin films codes are as V-Sn200, Sb-Sn200 and Ru-Sn200, respectively.

SAMPLES		Thickness (nm)	P (mN)	h (μm)	H (GPa)	E (GPa)
Films produced by SnO_2 target in the laboratory		L 50	0.1	0.0073	31.46±7.11	1150.51±141.80
		L 100	0.3	0.0130	21.70±2.63	867.98 ± 75.02
		L 200	0.5	0.0205	10.58±4.71	724.71±138.33
Films produced by purchased SnO_2 target in the laboratory		T 50	0.2	0.0086	29.38±8.22	1078.07±202.91
		T 100	0.3	0.0147	26.06±8.81	1052.97±194.02
		T 200	0.3	0.0218	17.31±4.30	819.86±121.51
Films produced by doped SnO_2 targets in the laboratory	Vanadium	V-Sn200	0.3	0.0208	41.07±7.82	553.07±139.61
	Rutenium	Ru-Sn200	0.3	0.0259	21.73±4.43	460.06±211.45
	Antimony	Sb-Sn200	0.3	0.0235	23.93±8.04	482.00±212.43

Table 1: Values of hardness (*H*). and elasticity modulus (*E*) of produced tin oxide films of 50. 100 and 200 nm thicknesses using laboratory lab-made and purchased SnO_2 targets

An increase in the depth of penetration was observed with the increase of the load. and elastoplastic behavior was observed here. These hardness and elasticity values are higher than normal macro vickers hardness values. due to the low number of dislocations. errors and defects in nano dimensions. T50. T100 and T200 coded samples has a high hardness and modulus of elasticity as mechanical properties. Compared to the others. the hardness value of vanadium additive films is the highest. The hardness of the doped samples with a thickness of 200 nm is show higher than the others.

These results are shown in Table 1 and Figure 12. Hardness values are between H = 10.580 - 41.076 GPa and the standard deviation is around 9%. It has been determined that they are mechanically durable materials. Elasticity modules were between 300-1200 GPa and the standard deviation was around 25%. As the indenter depth increased from the surface. the modulus of elasticity decreased. Nevertheless. the modulus of elasticity results are close to each other in these samples besides the modulus of elasticity being lower in the samples with doped [29].

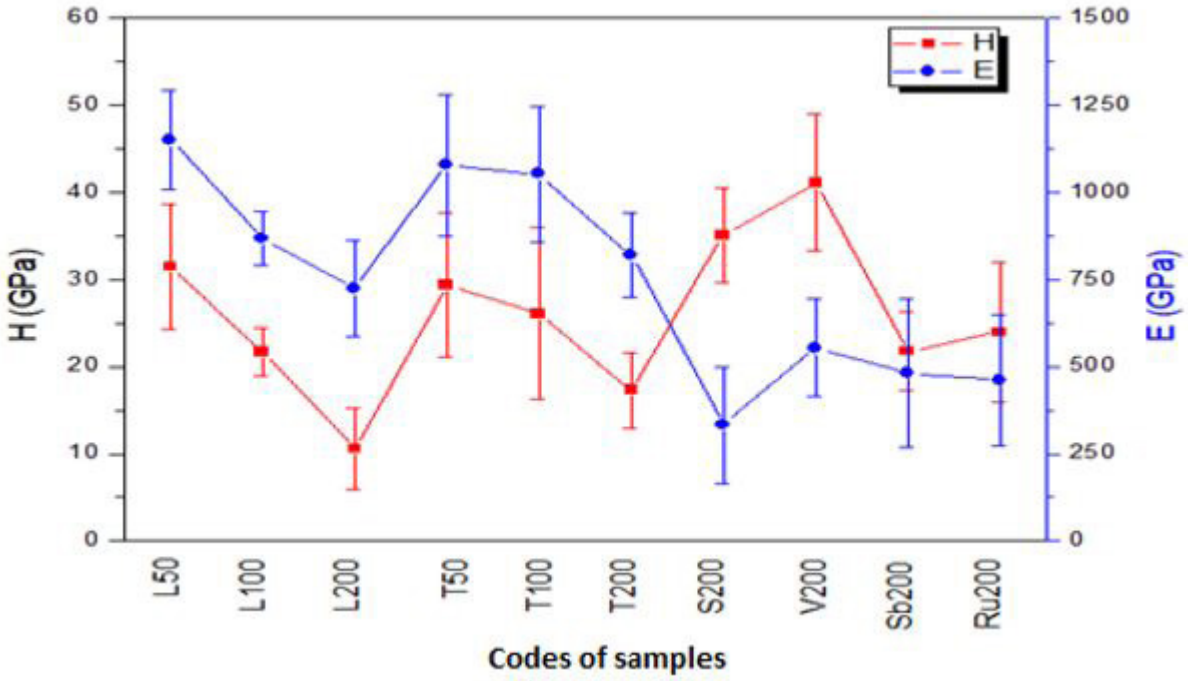

Figure 12: Hardness (*H*). and modulus of elasticity (*E*) graph from nanoindentation results of vanadium. antimony. ruthenium doped and undoped SnO_2 films in 50. 100 and 200 nm thicknesses

Electrical Properties

According to the optical properties of 200 nm thickness films. the band gap (BG) values of ruthenium. antimony. vanadium doped and undoped tin oxide thin films were calculated as 3.19 eV. 3.16 eV. 3.08 eV and 3.17 eV. respectively. as seen in Figure 13. The energy band gap values of the films clearly revealed the semiconducting nature of tin oxide. It was observed that the band gap energies of the films decreased from 3.6 eV to 3.08 eV with elemental doping. It turned out that the band gap values were lower than 3.6 eV for the SnO_2 films reported by Tiginyanu [30]. Zheng and Saipriya [21.26]. in their published article. argued that the band gap (eV) values of the films decrease as the annealing temperature increases. The reason for this decrease can be explained by the elimination of oxygen vacancies as a result of the annealing process. as well as the localization of intermediate oxygen atoms. Soltan et al. [31]. stated that with the addition of additive elements to pure tin oxide. the decrease in the band gap energy value accompanied the decrease in crystal size. According to the XRD patterns. it was observed that the doped and undoped films were well crystallized. Therefore. it is an expected result that the forbidden energy bands are different from each other. It revealed that the additives have an effect on the crystal structure band gap (Eg). Sankar et al. [17].. in their optical studies. revealed that the band gap energy decreases with increasing ruthenium concentrations. The opposite was observed with the addition of ruthenium. but there was slightly difference. Lee et al. [18]. noted that for vanadium and antimony doping resulted in an increase in carrier concentration and a decrease in Hall mobility. The band gap reduction of Sb-doped films is therefore expected.

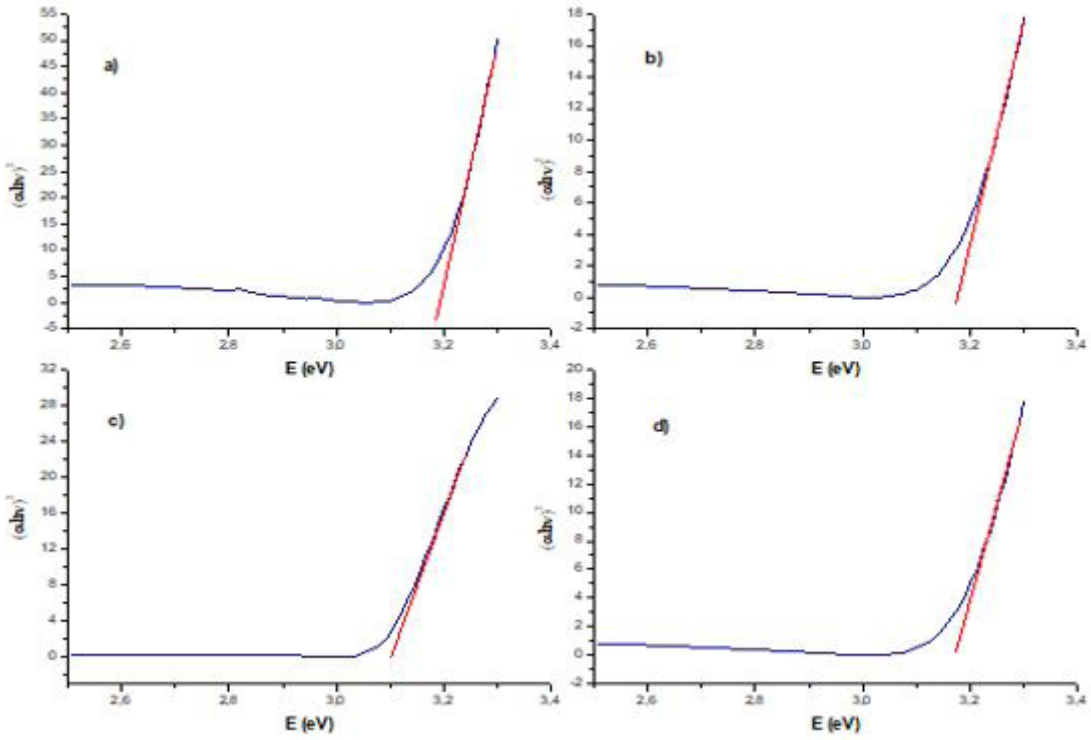

Figure 13: Band gap graphs of SnO_2 thin films produced in 200 nm thickness a) Ru-doped SnO_2 b) Sb-doped SnO_2 c) V-doped SnO_2 d) undoped SnO_2

Conclusions

In this study. tin oxide films were successfully coated on silica substrates by using doped and undoped targets and pellets by sputtering technique. After annealing. the films were characterized by analysis techniques.

An XRD phase analysis study was performed to compare the calcination temperatures and times of these thin films. The XRD diffraction patterns show that all the films are polycrystalline and the SnO tetragonal structure has peak features. It also increased with increasing annealing temperatures to increase the crystallinity of the films. It was observed that the crystalline dimensions of the films increased with increasing annealing temperature and time after the annealing temperature was increased from 550 °C to 650 °C. It has been observed that the optical properties change and the band gap energy decreases with increasing annealing temperature. The band gap values of all films as a function of annealing temperature were calculated in the range of 3.08 to 3.17 eV. When the XRD analysis results of all samples were examined. it was observed that the displacement of V. Ru and Sb atoms in the cassiterite lattice did not change the tin oxide cassiterite structure much. The crystal size of the doped films is in the order of 4-8 nm. The crystal size remained the same with the addition of vanadium. but tended to increase with the addition of Ru and Sb. We can conclude that the carbon (C) seen in the elemental analysis of all films is formed as hydrocarbon compounds (seen as standard) as a result of surface contamination. The binding energies of the valence bands of the films (Sn3d and O1s. C1s. V2p. Ru3d. Sb5d) were also presented by XPS analysis. In the elemental analysis results of the films. each additive was determined and it was observed that the binding energies for each increased. SEM and AFM results show that SnO2 thin films were successfully formed. SnO2 thin films appear relatively soft. but some cracks were seen on the film surface in some places. Particle sizes calculated using the Scherer formula (5-20) in SEM were found to be compatible. As can be seen from the SEM images. although not all films had very good morphology due to crack formation. they exhibited dense. well-crystallized ellipsoidal and spherical grains and a homogeneous and uniform crystalline structure with cracks and pores.

The bandgap (eV) energy gap appears to be about 3.10 eV for doped and undoped SnO2 films. These results show that the produced doped and undoped SnO2 films are semiconductor. Examination of the X-ray diffraction patterns revealed that the doped and undoped films crystallize well and that the additives have a remarkable effect on the crystal structure band gap (Eg).

According to the nanoindentation results. it was observed that the hardness value of the 200 nm thick vanadium-doped sample was compared with the others in the samples produced using the laboratory production target. While the stiffness is higher in doped thin film samples. the modulus of elasticity is close to each other. Due to the physical structure of the films in nanometric scale. high hardness values were obtained.

Acknowledgments

The authors cordially thank for financial and infrastructural supported by the Metallugy and Material Engineering Department by the Project of Dokuz Eylul University. BAP (Scientific Research Coordination Unit of DEU). (Project No: (2012.KB.FEN.025). The authors are indebted to State Planning Foundation (DPT) and Dokuz Eylul University for financial and infra-structural support forestablishment of Dokuz Eylul University. Center for Production and Applications of Electronic Materials (EMUM) where this research was carried out.

References

1. Pawar BG, Pinjari DV, Kolekar SS, Pandit AB, Han SH (2012) Effect of Sintering temperatures on the synthesis of SnO2 nanospheres. ISRN Chemical Engineering 954869: 7.

2. Shuping G, Jing X, Jianqiao L, Dongxiang Z (2008) Highly sensitive SnO2 thin film with low operating temperature prepared by sol–gel technique. Sensors and Actuators B 134: 57–61.

3. Sohn JC, Kim SE, Kim ZW, Yun SY (2009) H2S gas sensing properties of SnO2:CuO thin film sensors prepared by e-beam evaporation. Transactions on Electrical and Electronic Materials 10: 135-139.

4. Zribi A, Fortin J (2009) Functional thin films and nanostructures for sensors: Synthesis. physics and applications. Springer Science & Business Media. New York USA.

5. Gui T, Hao L, Wang J, Yuan L, Jia W, et al. (2010) Structure and features of SnO2 thin films prepared by RF reactive sputtering. Chinese Optics Letters 8: 134-136.

6. Wasa K, Kitabatake M, Adachi H (2004) Thin Film Materials Technology. Sputtering of Compound Materials. 115-189.

7. Liu S, Chen LY, Liu CY, Fang HW, Hsieh JH et al. (2011) Physical properties of polycrystalline Cr-doped SnO2 films grown on glasses using reactive DC magnetron co-sputtering technique. Applied Surface Science 257: 2254–2258.

8. Zampiceni E, Bontempi E, Sberveglieri G. Deper LE (2002) Mo influence on SnO2 thin films properties. Thin Solid Films 418: 16–20.

9. Kissine VV, Voroshilov SA, Sysoev VV (1999) A comparative study of SnO2 and SnO2:Cu thin films for gas sensor applications. Thin Solid Films 348: 304-311.

10. Ahn H, Noh JH, Kim SB, Overfelt RA, Yoon YS, et al.(2010) Effect of annealing and argon-to-oxygen ratio on sputtered SnO2 thin film sensor for ethylene gas detection. Materials Chemistry and Physics 124: 563–568.

11. Kim CK, Choi SM, Noh IH, Lee JH (2001) A Study on this gas sensor based on SnO2 prepared by pulsed laser deposition method. Sensors and Actuators B77: 463-467.

12. Wang Y, Ma C, Sun X, Li H (2002) Preparation and characterization of SnO2 nanoparticles with a surfactant mediated method. Nanotechnology 13: 565–569.

13. Cao X, Cao, L, Yao W, Ye X (1998) Influences of dopants on the electronic structure of SnO thin films. Thin Solid Films 317: 443–445.

14. Khan AF, Mehmooda M, Rana AM, Bhatti MT (2009) Effect of annealing on electrical resistivity of RF-magnetron sputtered nanostructured SnO2 thin films. Applied Surface Science 255: 8562–8565.

15. Yang H, Hu Y, Qiu G, (2002) Preparation of antimony-doped SnO2 nanocrystallites. Material Research Bulletin 37: 2453-2458.

16. Toloman D, Popa A, Raita O, Stan M, Suciu R, et al. (2014) Luminescent properties of vanadium-doped SnO2 nanoparticles.

Optical Materials 37: 223-228.

17. Sankar C, Ponnuswamy V, Manickam M, Mariappan R, Suresh R (2015) Structural. morphological. optical and gas sensing properties of pure and Ru doped SnO2 thin films by nebulizer spray pyrolysis technique. Applied Surface Science 349: 931-939.

18. Lee SY, Park BO (2006) Structural. electrical and optical characteristics of SnO2: Sb thin films by ultrasonic spray pyrolysis. Thin solid films 510(1-2): 154-158.

19. Kissine VV, Sysoev VV, Voroshilov SA (2001). Conductivity of SnO2 thin films in the presense of surface adsorbed spaces. Sensors and Actuators B 79: 163–170.

20. Kawabe T, Tabata K, Suzuki E, Ichikawa Y, Nagasawa Y (2001) The morphological effects of SnO2 thin film on catalytic activities and selectivities for te selective oxidation of CH4 metan. Catalysis Today 71: 21–29.

21. Saipriya S, Sultan M, Singh R (2011) Effect of environment and heat treatment on the optical properties of RF-sputtered SnO2 thin films. Physica B 406: 812-817.

22. Tas Anli S, Ebeoglugil ME, Celik E (2020) Effect of dopant elements on structure and morphology of SnO2 nanoparticles. Journal of the Australian Ceramic Society Volume 56 (2): 403-411.

23. Fisher-Cripps AC (2009). Nanoindentation (3rd ed.). Fischer-Cripps Laboratories Private company. Australia.

24. Moharrami N, Bull SJ (2014) A comparison of nanoindentation pile-up in bulk materials and thin films. Thin Solid Films 572: 189–199.

25. Reddy CV, Babu B, Vattikuti SP, Ravikumar RVSSN, Shim J (2016) Structural and optical properties of vanadium doped SnO2 nanoparticles with high photocatalytic activities. Journal of Luminescence 179: 26-34.

26. Zheng M, Ni J, Liang F, Wang MC, Zhao X (2016) Effect of annealing temperature on the crystalline structure. growth behaviour and properties of SnO2: Sb thin films prepared by radio frequency (RF)-magnetron sputtering. Journal of Alloys and Compounds 663: 371-378.

27. Sangeetha P, Sasirekha V, Ramakrishnan V (2011) Micro-raman investigation of tin dioxidenanos structured material based on annealing effect. Journal of Raman Spectroscopy 42: 1634–1639.

28. Oliver WC, Pharr GM (1992). An improved technique for determining hardness and elastic modulus using load and displacement sensing indentation experiments. Journal of Materials Research.7. 1564.

29. Kim GW, Sung CH, Seo YJ, Park KY, Heo SN, et al. (2012) Effect of dopants (Tri-valent. Penta-valent) on the electrical and optical properties of SnO2 based transparent electrodes. Journal of Ceramic Processing Research 13(2): 394-397.

30. Tiginyanu I, Topala P, Ursaki V (2016) Nanostructures and thin films for multifunctional applications. Technol. Eng. 183: 43–83.

31. Soltan WB, Mbarki M, Ammar S, Babot O, Toupance T (2016) Structural and optical properties of vanadium doped SnO2 nanoparticles synthesized by the polyol method. Optical Materials 54: 139-146.